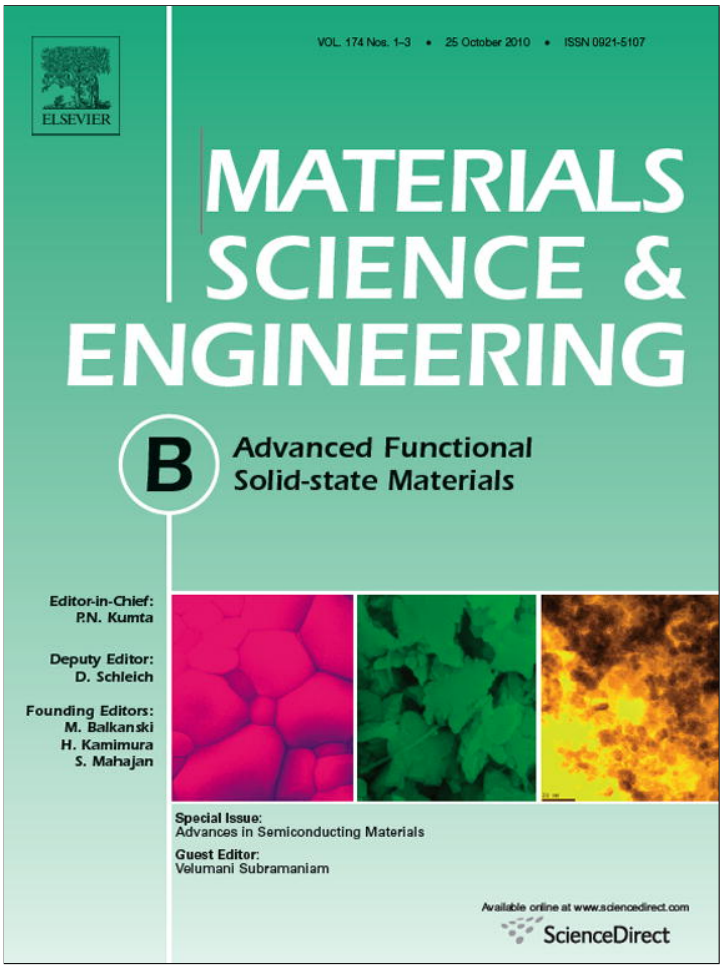

Materials Science and Engineering B 174 (2010) 13–17

Contents lists available at ScienceDirect

Materials Science and Engineering B

journal homepage: www.elsevier.com/locate/mseb

Decomposition of NO in gas phase by gold nanoparticles supported on titanium dioxide synthesized by the deposition–precipitation method

J. Hernández-Fernández[a,b,*], R. Zanella[c], A. Aguilar-Elguezabal[a], R.D. Arizabalo[b], S. Castillo[b], M. Moran-Pineda[b]

[a] Centro de Investigación en Materiales Avanzados, Av. Miguel de Cervantes 120, Complejo Industrial C.P. 31109, Chihuahua, Chih., Mexico
[b] Instituto Mexicano del Petróleo, Dirección de Investigación y Posgrado, Eje Central Lázaro Cárdenas 152, C.P. 07730, D.F., Mexico
[c] Centro de Ciencias Aplicadas y Desarrollo Tecnológico, UNAM, Circuito exterior S/N, Ciudad Universitaria, C.P. 04510, A.P. 70-186, Delegación Coyoacán, D.F., Mexico

ARTICLE INFO

Article history:
Received 1 September 2009
Received in revised form 6 February 2010
Accepted 10 March 2010

Keywords:
Titanium dioxide
Gold
Deposition–precipitation
Photocatalysis
Nitrogen monoxide

ABSTRACT

In the present work, the synthesis, characterization and photoactivity concerning the nitrogen monoxide (NO) decomposition of sol–gel Au/TiO_2 photocatalysts are reported. TiO_2 was prepared by gelling titanium (IV) isopropoxide, and gold nanoparticles were added by the deposition–precipitation method with urea. The catalysts with different gold concentrations were characterized by the following techniques: BET, XRD, UV–vis and dark-field TEM. It was found that by using this synthesis method, a high dispersion of gold nanoparticles on TiO_2 was reached (4.4–6.7 nm), and the obtained structure lead to a band gap energy that is lower than the one observed for undoped TiO_2. A NO + O_2 mixture (150 ppm) was used to evaluate the photocatalytic activity *in situ*, at room temperature, under atmospheric pressure and a UV lamp was used as radiation source. The photocatalytic conversion of nitrogen monoxide (NO) was followed by FTIR, which reached 96% in 60 min. The Au/TiO_2 materials showed an enhanced photocatalytic activity when compared with the reference TiO_2.

1. Introduction

TiO_2 has been considered as one of the most useful materials because of its high photoactivity, excellent optical transmittance, high refractive index, chemical inertness, stability against photochemical corrosion and cost-effectiveness [1,2]. Photon adsorption by TiO_2 results in the promotion of an electron from the valence band to the conduction band; the photoinduced electrons and positive charged holes can respectively reduce and oxidize the species adsorbed on the semiconductor surface [3]. In addition, the high rate of electron–hole recombination on TiO_2 particles is the major rate-limiting factor controlling the photocatalytic efficiency [4]. In order to increase the TiO_2 photocatalytic activity, the semiconductor has been modified by doping with transition metals or noble metals [5–8]. Among the different preparation methods to obtain gold nanoparticles supported on metallic oxides, the deposition–precipitation method with urea has been reported as one of the most efficient methods [9–10]. Au nanoparticles supported on titania in highly dispersed state exhibit a surprising high activity for several reactions such as low-temperature oxidation of CO, partial oxidation of hydrocarbons, and degradation of contaminants [11–14]. Nitrogen oxide gases (NO_x) are harmful air pollutants due to their role concerning not only the generation of photochemical smog and acid rain but also the promotion of the ozone formation [15]. For the decomposition of NO, different catalysts have been used: Cu–zeolites [16], PdO/Al_2O_3 [17], Rh/Al_2O_3 [18], Rh/SiO_2 [19], etc. The use of TiO_2 and Au/TiO_2 as photocatalyst for NO elimination has been scarcely studied in spite of the dual benefit that can be obtained with this system: the photocatalytic activity of TiO_2, and the NO adsorption on the Au nanoparticles [20,21]. The present study deals with the preparation of nanostructured Au/TiO_2 photocatalysts prepared by the deposition–precipitation method. The morphology, band gap energy and particle size of the obtained materials were analyzed. The photocatalytic activity of Au/TiO_2 was evaluated by the photocatalytic decomposition of NO, using an ultraviolet light source of 365 nm.

2. Experimental

2.1. Preparation of Au/TiO_2 nanoparticles

The TiO_2 used as a support was prepared by the sol–gel method from titanium tetraisopropoxide (Aldrich) mixed with 2-propanol (J.T. Baker 9000–03) and distilled water. The alkoxide hydrolysis

* Corresponding author at: Centro de Investigación en Materiales Avanzados, Av. Miguel de Cervantes 120, Complejo Industrial C.P. 31109, Chihuahua, Chih., Mexico.
E-mail address: javier.fernandez@cimav.edu.mx (J. Hernández-Fernández).

0921-5107/$ – see front matter © 2010 Elsevier B.V. All rights reserved.
doi:10.1016/j.mseb.2010.03.023

solution was adjusted at pH 3 by using hydrochloric acid. The solution was refluxed for 24 h at 70 °C under constant stirring until the gel was formed. Afterwards, the solids were dried in an oven for 12 h at 80 °C, using a 2 °C/min heating rate. The calcination of the materials was performed at 300 °C for 4.5 h. The gold deposition on the support was carried out by the deposition–precipitation method using urea, before preparation, TiO_2 was previously dried in air at 100 °C for at least 24 h. All of the preparations were performed in the absence of light, which is known to decompose the gold precursors. The support was mixed with a solution containing $HAuCl_4$ (4.2×10^{-3} M) (Aldrich 99.9%) and urea (0.42 M) (Aldrich 99.9%). The initial pH was ≈2. The suspension was heated at 80 °C and maintained under constant stirring for 16 h, in which progressive decomposition of urea in solution at temperature above 60 °C releases OH^- ions, which gradually increase the medium pH until it comes to a value of pH 8. This method makes possible the slow precipitation of hydroxides onto support, and avoids a brutal and local increase of pH, which could induce precipitation in solution. Regarding the preparation of supported gold catalysts, we observed that using the deposition–precipitation method with urea, almost all the gold in solution was deposited on the TiO_2 support [22]. After the deposition of gold onto TiO_2, the solids were separated from the precursor solution by centrifugation and washed several times with distilled water and dried under vacuum either at room temperature or 100 °C. The catalysts were reduced under hydrogen flow (100 ml/min) at 300 °C for 4 h. The gold content on catalysts was 0.3, 0.5, 0.7, 1.0 and 3.0 wt%, respectively.

2.2. Characterization of the catalysts

The specific surface area of the obtained materials was determined by the N_2 adsorption–desorption isotherms by means of a Quantachrome Autosorb 3B sorptometer. The specific surface area was calculated from the adsorption isotherms by the BET equation. The crystalline phase was determined by X-ray diffraction (XRD) with a Bruker D-8 diffractometer using Cu Kα radiation with a 2θ step of 0.03. The transmission electron microscopy studies (TEM) were performed on a JEM-2200FS equipment with an acceleration voltage of 200 kV. High-angle annular dark-field scanning transmission electron microscopy (HAADF-STEM) was also performed. The local chemical analysis and the chemical mapping were performed by means of an Energy-Dispersion X-ray spectrometer (EDXS) NORAN, which was coupled to a microscope allowing the STEM-EDX combination. The UV–vis spectra (200–900 nm) of the materials were obtained with an UV–vis Varian Cary 100 spectrophotometer (diffuse reflectance).

2.3. Evaluation of the photocatalytic activity

The evaluation of the photocatalytic activity was performed *in situ* by means of a Bruker IFS66 v/s spectrometer equipped with an MCT (Mercury–Cadmium–Tellurium) high sensitivity detector with a resolution of 0.5 cm^{-1} and an optical step of 25 cm^{-1}. The obtained materials were placed within a photocatalytic reactor (designed in our laboratory) with a length of 20 cm and potassium bromide (KBr) windows on its opposite sides in order to obtain real-time measurements. The UV lamp (Pen–Ray from UVP Corporation and wavelength of 365 nm) was used for irradiation; the lamp was horizontally placed at the upper part of the reactor, 10 cm from both ends. Fig. 1 shows the schematic representation of the photocatalytic reactor system used in the evaluation of the photocatalytic activity. The evaluation was carried out by using 100 mg of catalyst; reaction time was 60 min and tests were made at atmospheric pressure and room temperature. The system also has a vacuum system to remove the gases from the cell before photocatalytic test, and an air purge system that creates a clean atmosphere inside the photocatalytic reactor chamber. A NO–O_2 mixture was admitted with a concentration of NO of 150 ppm. The IR spectra were taken within the range from 4000 to 400 cm^{-1}, and monitored every 4 min.

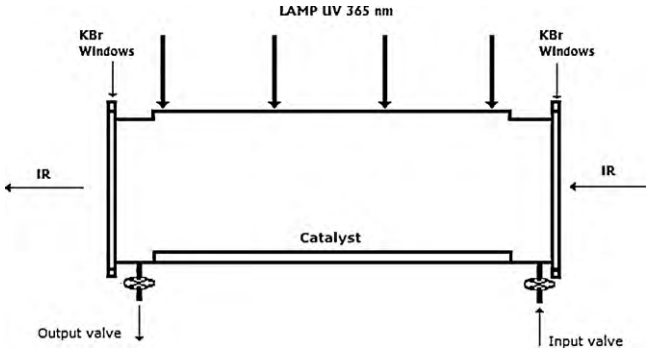

Fig. 1. Scheme of the photocatalytic reactor system.

3. Results and discussion

In Table 1 we observe the Au particle average diameter, BET, E_g and NO removal after 60 min. As we can see, when the gold concentration increases, the conversion diminishes, which can be correlated with the increase of the particle size, thus as the particle size increases, the photocatalytic activity decreases. In the Au concentration interval from 0.3 to 0.7 wt% the particle diameter remains around 4.7 nm, then, we would not expect that an Au percentage of 0.2 wt% or lower could lead to a different photocatalytic activity by this method of Au/TiO_2 synthesis.

The photocatalyst used as reference presented a surface area of 162 m^2/g, this value is maintained almost constant the Au deposition, independently of the gold content. This stability can be explained due to the calcination treatment at 300 °C, which allows the definition of the structure, and the process by which the gold was deposited requires temperatures lower than 80 °C. In the case of the band gap energy, we can observe that as the amount of gold increases on TiO_2, E_g diminishes, which coincides with the apparition of the plasmon, observed in Fig. 3.

The X-ray patterns are shown in Fig. 2. These spectra are in good agreement with the reference patterns, of titanium dioxide and gold (JCPDS 21-1272, 21-1276, 76-1934 and 652870) for the catalysts after reduction under hydrogen flow at 300 °C. The spectra show the characteristic diffraction peaks of titania anatase phase and a peak assigned to the brookite phase ($2\theta = 31°$). The diffraction

Table 1
Au particle average diameter, specific surface areas, band gap energy and photocatalytic activity of the studied materials.

Catalyst	Average Au diameter [nm]	BET [m^2/g]	E_g [eV]	NO removal after 60 min [%]
TiO_2	–	161	3.13	70
Au/TiO_2 0.3%	4.6	157	3.09	96
Au/TiO_2 0.5%	4.6	158	3.03	95
Au/TiO_2 0.7%	4.7	156	2.96	95
Au/TiO_2 1.0%	5.7	161	2.95	88
Au/TiO_2 3.0%	6.7	155	2.64	85

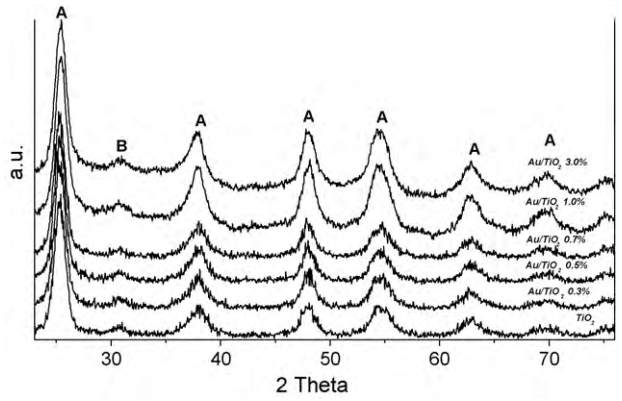

Fig. 2. X-ray diffraction patterns of the materials. Reflections due to anatase and brookite are labeled as (A) and (B), respectively.

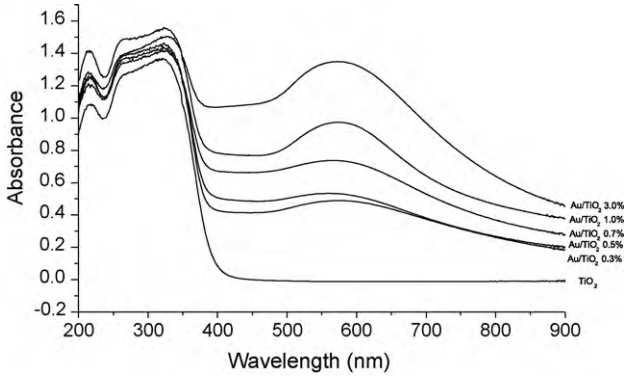

Fig. 3. Diffuse reflectance spectra of Au/TiO_2 photocatalysts and bare TiO_2 prepared at different Au concentrations.

patterns show the anatase crystalline phase in a higher proportion with respect to that of brookite. It must be noted that the peaks corresponding to Au^0 ($2\theta = 38.18, 44.39, 64.57$) are not clearly observed, which suggests that gold is present as nanosized-gold particles whose size is below 10 nm. The low Au content (0.3, 0.5, 0.7, 1.0 and 3.0 wt%) in addition to the small size of the gold particles did not allow their detection by this technique [23].

The diffuse reflectance spectra for the materials are shown in Fig. 3. The band gap energy values obtained in this way for the bare and doped TiO_2 materials are summarized in Table 1. The TiO_2 absorption peak appears in the 391 nm region, the band widening in the 520–680 nm region is characteristic of the plasmon resonance of metallic gold particles. For metal nanoparticles of Au^0, Cu^0, and Ag^0, the plasmon absorption arises from the collective oscillations of the free conduction band electrons that are induced by the incident electromagnetic radiation [24].

In Fig. 4(a–c) representative images of the Au/TiO_2 (0.3, 0.5, 0.7 wt%) after calcination are shown. These composite nanoparticles are spherical in shape. Due to the low concentration of the metal capping, we expect that the size and distribution of the nanocomposite particles remain ruled by the TiO_2 nanoparticles characteristics. The particle diameter of gold-capped TiO_2 nanoparticles was in the range of 4.4–6.7 nm. The gold particles can be observed as small white spots which are in contrast with the support. The high surface area provided by TiO_2 particles allowed the

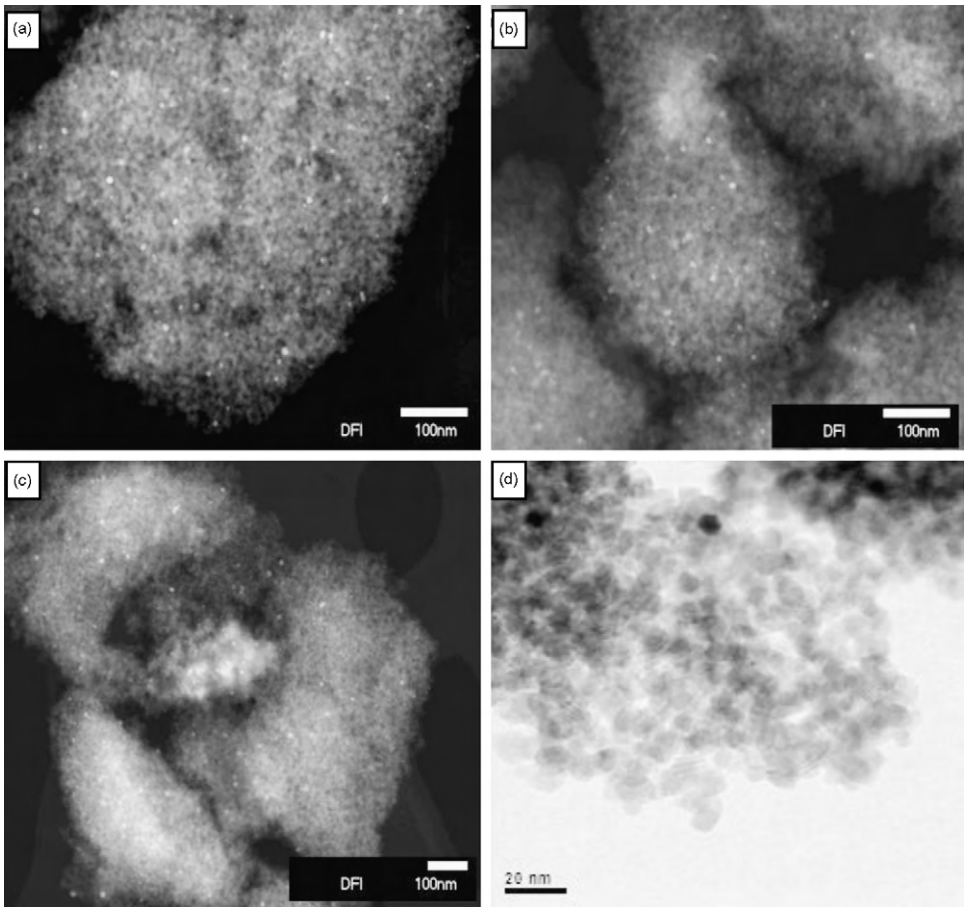

Fig. 4. HAADF image for: (a) Au/TiO_2 0.3 wt%, (b) Au/TiO_2 0.5 wt%, (c) Au/TiO_2 0.7 wt%, and (d) HRTEM TiO_2 support.

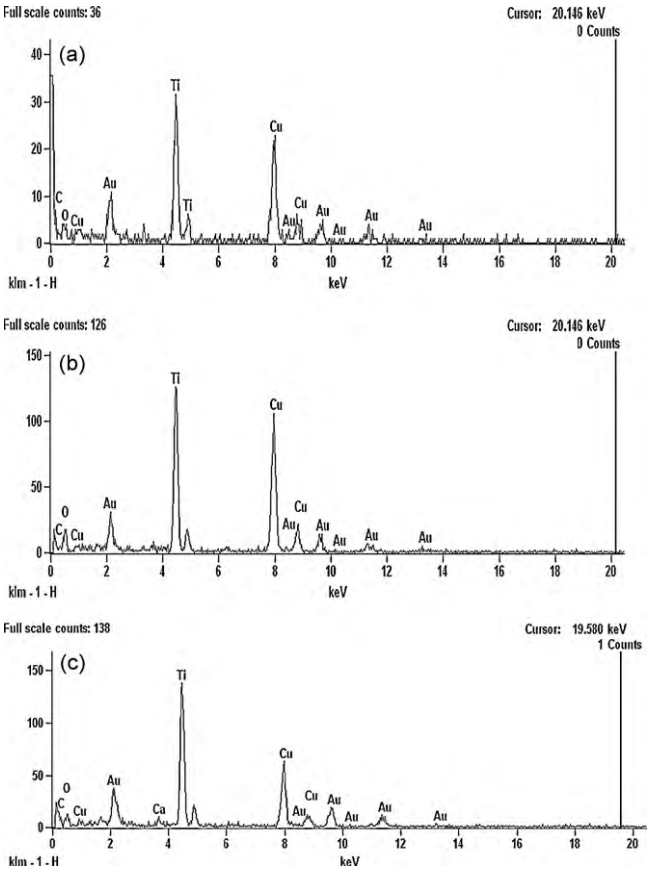

Fig. 5. EDX for: (a) Au/TiO_2 0.3 wt%, (b) Au/TiO_2 0.5 wt% and (c) Au/TiO_2 0.7 wt%.

high dispersion of Au particles and by this way the restrain of Au particle growth, since we do not see significant growth in the size of Au nanoparticles. The small size of the gold particles implies that a strong interaction occurs between the TiO_2 support and the gold precipitate during the deposition, which leads to a high dispersion of metallic gold. Fig. 4(d) shows the HRTEM image of different nanoparticles of the TiO_2 support with an average size of 12 nm.

The EDX patterns, Fig. 5, of the Au/TiO_2 particles present the four X-ray lines that are associated with O Kα, Au Kα, Ti Kα, and Cu Kα. Cu Kα line corresponds to the copper grid used for the TEM analysis. The results indicate that Ti, O and Au are the constitutive elements of the nanoparticles.

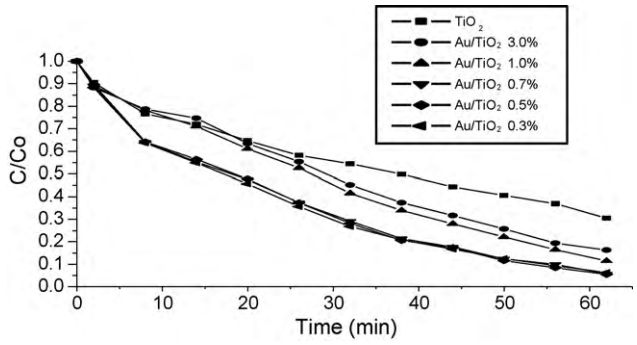

Fig. 6. Profile of the percentage of nitric oxide decomposition by the Au/TiO_2 and TiO_2 photocatalysts as a time function during photocatalytic activity tests.

The three nitrogen oxides: N_2O (nitrous oxide), NO (nitric oxide) and NO_2 (nitrogen dioxide) present IR absorption bands at 2225, 1875 and 1607 cm^{-1}, respectively [25]. The change in the concentration of NO in an oxygen-rich atmosphere was recorded as a function of time. The result of our study shows that there is an appreciable increase in the photocatalytic activity. It can be seen that the Au/TiO_2 (0.3 wt%) catalyst shows a conversion of 96%, the Au/TiO_2 (1.0 wt%) 88%, the Au/TiO_2 (3.0 wt%) 85%; and the bare TiO_2 70% (Fig. 6). The analysis of the stoichiometric balance indicates that the main reaction deals with the NO reduction to form N_2 and O_2; and some formation of N_2O was found according to IR spectra (Fig. 7), and the formation of NO_2 is not observed, the presence of N_2 and O_2 cannot be determined by this technique. These results are according to the reaction path proposed by Bowering et al. [26], who considers the following reactions:

$$TiO_2 + h\upsilon \rightarrow e^- + h^+ \quad (1)$$

$$NO + e^- \rightarrow N + O \quad (2)$$

$$NO + N \rightarrow N_2O \quad (3)$$

$$NO + O \rightarrow NO_2 \quad (4)$$

$$2O \rightarrow O_2 \quad (5)$$

$$2N \rightarrow N_2 \quad (6)$$

$$2NO \rightarrow N_2 + O_2 \quad (7)$$

$$N_2O \rightarrow N_2 + O \quad (8)$$

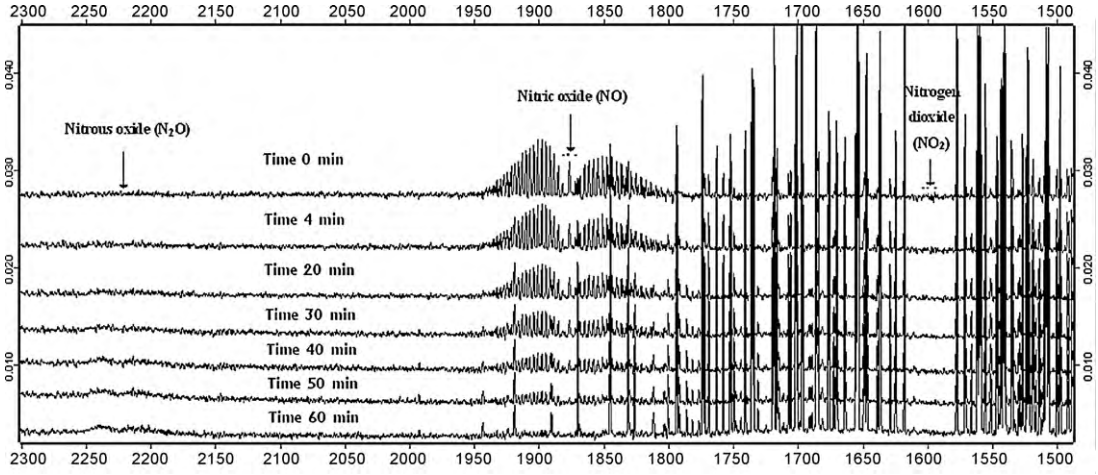

Fig. 7. FTIR-spectra for NO decomposition over Au/TiO_2 as a function of time in a typical photocatalytic degradation test.

In our photocatalytic tests, the reaction number (4) does not seem to occur, and the formation of N_2O, as described in reaction number (3) seems to be prevalent.

A great number of variables can play simultaneously important roles in the NO decomposition. According to the photocatalytic activity, the highest reactivity seems to be mainly related to the pure anatase phase of the sample, the specific surface area and the gold particles in the nanometric range. The presence of Au on the surface of TiO_2 improves the photocatalytic activity of TiO_2. The role of the gold particles can be in several ways associated with the decrease of the e^-/h^+ pair recombination rate, which improves the photocatalytic activity, a higher interaction of NO with the catalyst surface and the displacement of the band gap to lower energy values.

4. Conclusions

In the present work, we have prepared Au/TiO_2 catalysts by the deposition–precipitation with urea. The gold loadings were different: 0.3, 0.5, 0.7, 1.0 and 3.0 wt% and the size of Au particles were in the range of 4.4–6.7 nm, and highly disperse on TiO_2. It was found that gold shifts the band gap energy to lower energy values. A direct correlation between the gold content and the plasmon intensity band was observed in the UV–vis spectra. It was shown that more efficient photocatalysts for the NO decomposition can be obtained by depositing gold nanoparticles on TiO_2 supports. Under the reaction condition of this work, the best Au content was around 0.3 wt%, with a conversion of 96%.

Acknowledgments

The authors want to thank the support provided by the Instituto Mexicano del Petróleo (IMP) and Consejo Nacional de Ciencia y Tecnología (CONACYT).

References

[1] Y. Zhao, C. Li, X. Liu, F. Gu, H. Jiang, W. Shao, L. Zhang, Y. Li, Mater. Lett. 61 (2007) 79–83.
[2] Y. Lin, Mater. Lett. 62 (2008) 1246–1248.
[3] A.G. Agrios, P. Pichat, J. Appl. Electrochem. 35 (2005) 655–663.
[4] V. Iliev, D. Tomova, L. Bilyarska, G. Tyuliev, J. Mol. Catal. A: Chem. 263 (2007) 32–38.
[5] M.S. Park, M. Kang, Mater. Lett. 62 (2008) 183–187.
[6] K. Wilke, H.D. Breuer, J. Photochem. Photobiol. A: Chem. 121 (1999) 49–53.
[7] T. López, V.J. Hernández, R. Gómez, F. Tzompantzi, E. Sánchez, X. Bokhimi, A. García, J. Mol. Catal. A: Chem. 167 (2001) 101–107.
[8] M.H. Khedr, K.S. Halim, N.K. Soliman, Mater. Lett. 63 (2009) 598–601.
[9] M. Haruta, CATTECH 6 (2002) 102–115.
[10] X. Wang, H. Kawanami, S.E. Dapurkar, N.S. Venkataramanan, M. Chatterjee, T. Yokoyama, Y. Ikushima, Appl. Catal. A: Gen. 349 (2008) 86–90.
[11] A. Orlov, D.A. Jefferson, M. Tikhov, R.M. Lambert, Catal. Commun. 8 (2007) 821–824.
[12] C.N. Kuo, H.F. Chen, J.N. Lin, B.Z. Wan, Catal. Today 122 (2007) 270–276.
[13] C. Cellier, S. Lambert, E.M. Gaigneaux, C. Poleunis, V. Ruaux, P. Eloy, C. Lahousse, P. Bertrand, J.P. Pirard, P. Grange, Appl. Catal. B: Environ. 70 (2007) 406–416.
[14] T. Diemant, H. Hartmann, J. Bansmann, R.J. Behm, J. Catal. 252 (2007) 171–177.
[15] F.B. Li, X.Z. Li, C.H. Ao, M.F. Hou, S.C. Lee, Appl. Catal. B: Environ. 54 (2004) 275–283.
[16] P. Smeets, M.H. Groothaert, R.M. Van Teeffelen, H. Leeman, E.J.M. Hensen, R.A. Schoonheydt, J. Catal. 245 (2007) 358–368.
[17] Y.-J. Huang, H.P. Wang, C.-T. Yeh, C.C. Tai, C.Y. Peng, Chemosphere 39 (1999) 2279–2287.
[18] K. Almusaiteer, R. Krishnamurthy, S.S.C. Chuang, Catal. Today 55 (2000) 291–299.
[19] H. Papp, D.P. Sabde, Appl. Catal. B: Environ. 60 (2005) 65–71.
[20] M.A. Debeila, N.J. Coville, M.S. Scurrell, G.R. Hearne, M.J. Witcomb, J. Phys. Chem. B 108 (2004) 18524–18560.
[21] J. Zhang, T. Asuyama, M. Minagawa, K. Kinugawa, H. Yamashita, M. Matsuoka, M. Anpo, J. Catal. 198 (2002) 1–8.
[22] R. Zanella, L. Delannoy, C. Louis, Appl. Catal. A: Gen. 291 (2005) 62–72.
[23] C. Guzmán, G. Del Angel, R. Gómez, F. Galindo, R. Zanella, G. Torres, C. Ángeles, J.L.G. Fierro, J. Nanopart. Res. 5 (2009) 13–23.
[24] R. Zanella, S. Giorgio, C.H. Shin, C.R. Henry, C. Louis, J. Catal. 222 (2004) 357–367.
[25] B. Ganemi, E. Bjornbom, J. Paul, Appl. Catal. B: Environ. 17 (1998) 293–311.
[26] N. Bowering, G.S. Walter, P.G. Harrison, Appl. Catal. B: Environ. 62 (2006) 208–216.